Vol 13 No 12, December 2004
1009-1963/2004/13(12)/2115-06

Chinese Physics

© 2004 Chin. Phys. Soc.
and IOP Publishing Ltd

# Modelling of an obliquely deposited thin film in three dimensions by kinetic Monte Carlo method*

Liu Zu-Li(刘祖黎)†, Zhang Xue-Feng(张雪锋), Yao Kai-Lun(姚凯伦), Wei He-Lin(魏合林), and Huang Yun-Mi(黄运米)

*Department of Physics, Huazhong University of Science and Technology, Wuhan* 430074, *China*

(Received 29 April 2004; revised manuscript received 12 July 2004)

A simulation of the growth of an obliquely deposited thin film in a three-dimensional lattice was made using kinetic Monte Carlo method. Cu growth in three dimensions on a (001) substrate with high deposition rates has been simulated in this model. We mainly investigated the variation of three-dimensional morphology and microstructure of films with incidence angle of sputtered flux. The relation of roughness and densities of films with incidence angle was also investigated. The simulation results show that the surface roughness increases and the relative density of thin film decreases with increasing incidence angle, respectively; the columnar structures were separated by void regions for large incidence angle and high deposition rate. The simulation results are in good agreement with experimental results. However, the orientation angle of columns is not completely consistent with the classical tangent rule.

**Keywords:** kinetic Monte Carlo method, oblique deposition, three-dimensional morphology, microstructure

**PACC:** 6855, 8110B, 8110F, 8250J

## 1. Introduction

A considerable number of theoretical and experimental studies are focused on film growth. Thin films are widely used in modern optical and electric devices. Many properties of opto-electronic thin film depend on the film morphology, texture and microstructure. For example, the large grains can restrain electromigration of metal interconnections[1] in a very large-scale integrated circuit. On the other hand, films with voids or columns are sometimes desirable because of their anisotropic electromagnetic and optical properties.[2,3] The morphology and the microstructure of films are determined by the growing process at the atomic-scale. So the simulation of thin film growth based on the atomic-scale model attracts considerable attention. A diffusion-limited aggregation (DLA) model[4] is an earlier Monte Carlo (MC) model for film growth but the deposition rate and temperature parameters are not included. Bruschi[5] proposed a two-dimensional (2D) MC model, which incorporated the deposition process and surface diffusion process together. Wei *et al* [6−8] studied the effect of the substrate temperature and deposition rate on the growth process of the thin film in some detail. To study the microstructure and texture of a thin film, a three-dimensional (3D) model is proposed in this paper. The solid on solid (SOS) model[9] (see Fig.1) is a coarse 3D model, which is suitable for the simulation of film growth using molecular beam epitaxy. Nevertheless, the crystalline lattice structure is not considered and the over-hangs (protruding atoms on the edge of a terrace) are not allowed in this model. The ballistic deposition model[10,11] is devised to simulate the sputtering deposition, but the surface diffusion process is too simple. Recently, Huang and Gilmer[12,13] presented a 3D simulator known as ADEPT using the so-called lattice Monte Carlo method. They successfully simulated the features of aluminum films deposited onto trenches and vias. Deposition at high rate and moderate temperature may cause formation of columnar structure. In

*Project supported by the National Natural Science Foundation of China (Grant Nos 10174023 and 90103034).
†E-mail: zxf1228@163.com and zlliu@hust.edu.cn

addition, an oblique angle of incidence can also lead to columnar film morphology.[14] For example, when particles arrive at the sidewalls of trenches or vias, columns or voids will be formed.[12]

In this article, we propose a 3D model using the kinetic Monte Carlo (KMC) method, in which the processes of deposition and diffusion are included. Compared with the earlier models, our model is really a 3D one and the lattice structure of the simulated material is also considered. Here, we mainly investigate the effect of oblique incidence of atom flux on the surface roughness, relative density, morphology and microstructure of Cu films deposited on a Cu(001) substrate.

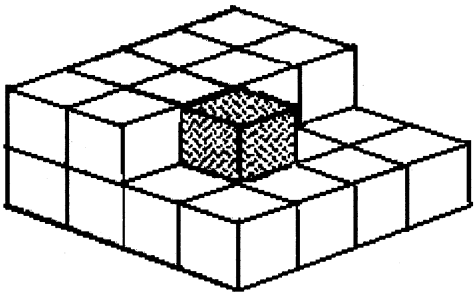


**Fig.1.** The solid on solid model in Ref.[9].

## 2. The model

In this paper, the simulation of deposition Cu onto a Cu(001) surface is carried out and the 3D mesh corresponding to the fcc lattice structure of Cu is built. In the following KMC simulations, atoms are constrained to remain at their discrete lattice sites. This is a valid assumption when the temperature is lower than about $0.5T_{\mathrm{m}}$ (melting point), since atomic motion is largely restricted to vibrations about lattice sites.[15] The substrate is periodic in the lateral direction and open in the vertical direction. An incident atom is selected with random lateral coordinates in the sputtering target above the substrate. The trajectory of the atom is chosen with a random azimuthal angle $\varphi$ and a particular polar angle $\theta$, where $\varphi$ ranges from 0 to $2\pi$. The polar angle $\theta$ is chosen as some specific values ($\theta$ ranging from 0 to $\pi/2$). The incident atom travels to the substrate along a line with starting angles $\varphi$ and $\theta$ (see Fig.2). A site with the highest coordination number, found among those sites near the trajectory within one lattice spacing, will be occupied by the new incident atom.

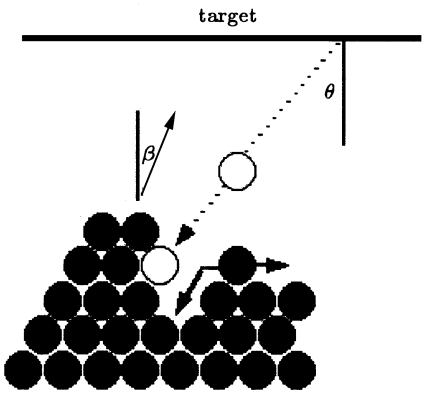



**Fig.2.** 2D sketch map showing the deposition process in the model. $\theta$ is the incidence angle of atoms and $\beta$ is the column orientation angle (inclined angle of the column). The arrows indicate possible diffusion directions of adatoms.

The lattice site with three or more nearest neighbouring atoms is considered to be stable, which is called "stable site" in the text and can be occupied by an atom. However, not all stable sites can be occupied by an atom on considering the arrangement of the nearest neighbouring atoms. In Fig.3, the dark circles represent the atoms below, the light gray ones the atoms above and the white ones the empty sites. The arrows indicate the possible jump directions of an atom. Atom 2 is not stable although it has three nearest neighbours, because there is a low energy barrier with which it easily falls down along the arrow direction.[16] Compared with atom 2, atom 1 is considered to be stable because it is not only on a (001) plane, but also on a (111) facet of fcc lattice. Likewise, it also has three nearest atoms. Thus, protruding atoms (over-hangs) are permitted in the model. This is different from the earlier MC model where no such

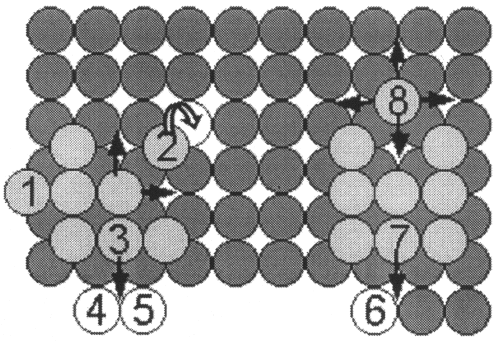



**Fig.3.** Sketch showing surface diffusion. The arrows indicate possible diffusion directions of adatoms. The dark circles represent the atoms below, the light gray ones the atoms above and the white ones the empty sites. Atom 2 is not stable and easily falls down to the lower empty site along the arrow direction. Atom 1 sits on the (111) plane of fcc lattice. Atom 3 can overcome the Ehrlich–Schwoebel barrier and jump to site 4 or 5, likely atom 7 to site 6.

atoms were allowed.[8] The experiments also show that these protruding atoms exist under certain conditions, such as when metal atoms are deposited onto trenches and vias.[12,13]

In the deposition process, an atom buried under newly arriving atoms is considered to be a "bulk atom", which cannot diffuse any more. In order to store the diffusion rates and coordinates of movable atoms, a hashing array is constructed, in which the jump rate and coordinates of movable atoms are both stored. The diffusion rates (or jump rate) of a single adatom was defined as the probability of a diffusion jump per unit time and is given by the Arrhenius-type expression

$$\nu = \nu_0 \exp(-E_{\mathrm{B}}/kT), \tag{1}$$

where $\nu_0 = 10^{12}\mathrm{s}^{-1}$ is the commonly-used attempt rate, $k$ is the Boltzmann constant, $T$ is the substrate temperature ($T$ is held at 300K in our simulation) and $E_{\mathrm{B}}$ is the activation barrier. Then the rates and coordinates of atoms are pushed into the hashing array. The event of inserting a new atom or surface diffusion is randomly chosen according to the ratio of the deposition rate to the total rate of all events. If a diffusion event takes place, an atom is selected and a jump to an empty neighbour site is performed. The pairwise potential energy of the Born–Mayer type[17,18]

$$E_i = -\left\{\sum_j \xi^2 \exp(-2q(r_{ij}/r_0 - 1))\right\}^{1/2} + \sum_j A\exp[-p(r_{ij}/r_0 - 1)], \tag{2}$$

is used to model the interaction between two atoms, where $\xi$ is an effective hopping integral, $r_{ij}$ is the distance between atoms $i$ and $j$, $r_0$ is the nearest neighbour distance, and the four parameters $\xi$, $q$, $A$, $p$ are determined by experimental data of the cohesive energy, the lattice parameter, the bulk modulus and the elastic constants, respectively. In this article, the parameters are listed in Table 1.

**Table 1.** The parameters used in our simulation to calculate the activation barrier.

| parameters | $\xi$/eV | $q$ | $A$/eV | $p$ | $r_0$/nm | $r_{i,j}$ |
|---|---|---|---|---|---|---|
| Cu-Cu | 1.224 | 2.278 | 0.0855 | 10.960 | 0.2556 | $< 1.5r_0$ |

The algorithm is summarized as follows: (1) the jump rates of all movable atoms are calculated and pushed into the hashing array. (2) The event of deposition or diffusion is determined by comparing the ratio $p = \dfrac{V_{\mathrm{d}}}{V_{\mathrm{d}} + R_{\mathrm{h}}}$ with a random number $\xi_1$ in the interval (0, 1), where $V_d$ is the deposition rate and $R_{\mathrm{h}}$ is the total diffusion rate of atoms. If $\xi < p$, the event of deposition is chosen, a new atom is inserted in an empty stable site, otherwise, the diffusion event is chosen. (3) A diffusion atom $M$ is chosen according to $\sum_{j=1}^{M-1} \nu_j < \xi_2 R_{\mathrm{h}} \leq \sum_{j=1}^{M} \nu_j$, where $\xi_2$ is a random number, $R_{\mathrm{h}}$ is total diffusion rate of atoms, the $\nu_j = \sum_{k=1}^{n} \nu_j^k$ is the jump rate of the $j$th atom, $n$ is the total possible diffusion directions of the $j$th atom and $\nu_j^k$ is the $k$th directional jump rate of the $j$th atom, which is calculated with formula $\nu_j^k = \nu_0 \exp(-E_{\mathrm{B}}^{(k)}/kT)$ and $E_{\mathrm{B}}^k$ is the diffusion barrier of this atom in the $k$th direction. (4) Move the atom $M$ to the new site specified by diffusion event. (5) Update the diffusion rates for the affected atoms. (6) The jump rates of affected atoms are re-calculated and the hashing array is updated. Then a new cycle starts.

## 3. Results and discussion

Figures 4(a) and (b) show the 3D morphologies and their 2D sections for films deposited onto a Cu(001) substrate at different incidence angles, where the deposition rate is chosen to be 10nm/min. For $\theta = 0°$, the surface looks smoother and only a few columns appear, and the thickness of the film is less than that for other incidence angles, indicating that few voids exist in the film under this incidence angle. In the case of $\theta = 30°$, some larger columns are formed, which are inclined toward the atom impinging direction (incident direction) and the inclined angle $\beta$ is small ($\beta$ is defined as the column orientation angle, see Fig.2). For $\theta = 60°$, the columns become higher and the inclined angle $\beta$ becomes larger. The region of voids between columns becomes larger than that in the case of $\theta = 30°$. Some facets appear on the side face of the columns. Finally, the columns are almost completely separated by some large void regions; the (111) facets become larger and can be seen clearly when $\theta = 75°$, because the (111) facet is the low index plane in a fcc crystal. The formation of columns and voids in the film has been explained as a kinetic roughening mechanism.[19,20] In the case of impinging atoms arriving at large incidence angles, the hills formed by previously deposited atoms intercept more atom flux to arrive the valley behind them. At the same time, the low mobility prevents atoms from moving to the valley and the ultimate outcome is the formation of the columnar structure in the films as shown in Fig.4.

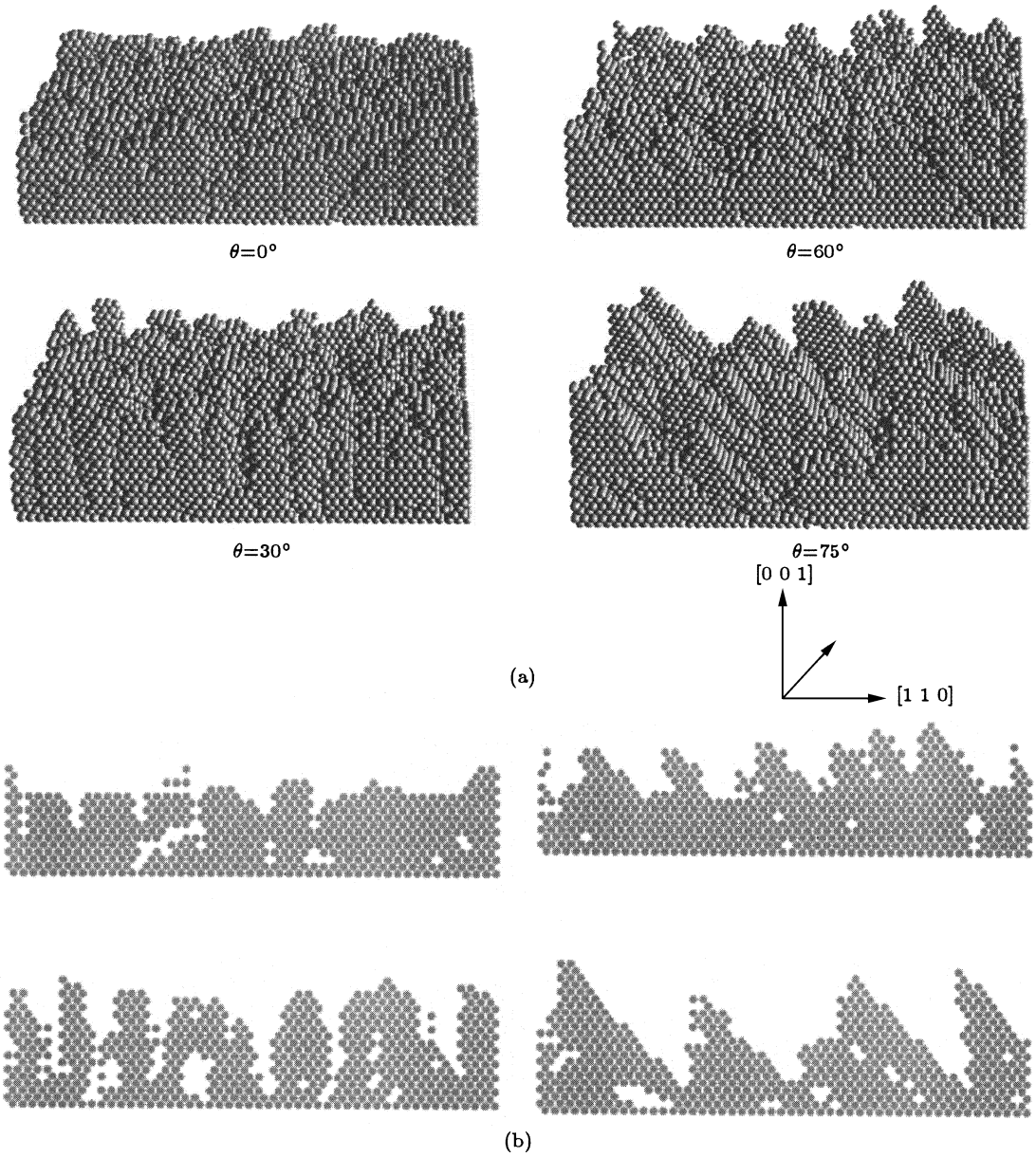



**Fig.4.** (a) 3D morphology variation as a function of incidence angle $\theta = 0°$, $30°$, $60°$ and $75°$. (b) The 2D sections of a two layers thickness from the 3D simulation. The deposition rate is 10nm/min and the temperature $T$ is 300K.

The variation of the inclined angle ($\beta$) with incidence angle ($\theta$) can be seen in Fig.4 (b). For $\theta = 0°$, the columns are basically vertical to the substrate. For $\theta = 30°$, the columns are slightly inclined toward the incident direction, but we find that the inclined direction of the column does not coincide with the incidence angle ($\theta$). For other cases, the inclined angle ($\beta$) becomes larger when the incidence angle ($\theta$) is larger. In our simulation, for incidence angles $\theta = 30°, 60°$ and $75°$, the corresponding average values of the angles ($\beta$) of growth for columns are about $10.5°, 34°$ and $45°$, respectively, where

$$\beta = \tan^{-1}(R^{-1}), \tag{3}$$

$$R = \langle z_i - z_0 \rangle / \langle x_i - x_0 \rangle, \tag{4}$$

$$\langle x_i - x_0 \rangle = \frac{1}{N} \sum_i^N (x_i - x_0), \tag{5}$$

$$\langle z_i - z_0 \rangle = \frac{1}{N} \sum_i^N (z_i - z_0), \tag{6}$$

$N$ is the number of the counted particles, $x_i$ and $z_i$ are the coordinates of the $i$th particle in a slice of the 3D film, and $x_{i0}$ and $z_{i0}$ are the coordinates of the first particle in the group which contains the $i$th particle (see Ref.[11]). From the values of these angles, it seems that the column growth angle $\beta$ and the incidence angle $\theta$ are not in accordance with the tangent

rule (i.e. $\tan(\beta) = \frac{1}{2}\tan(\theta)$).[14,20,21] The reason is that the atoms are attached at the step edge to produce overhanging configurations, leading to small inclined angles of columns.[13] The relation between the incidence angle and the inclined angle of the column is plotted in Fig.5.

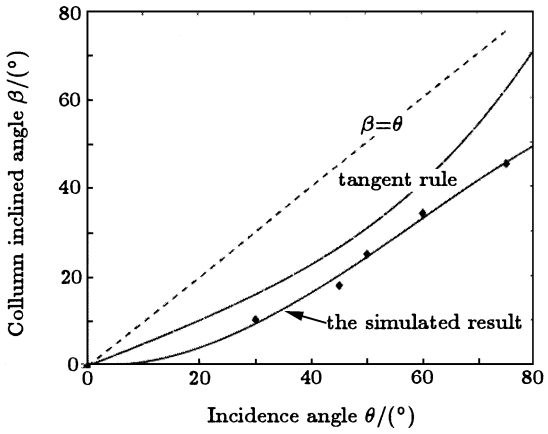



**Fig.5.** The relation between the incidence angle and the column inclined angle. The simulated results are plotted in solid line with diamond marks. For comparison, $\beta = \alpha$ (dotted line) and the tangent rule line are also plotted (dashed curve).

In order to characterize the films, we define the roughness $\sigma$ and the relative density of the film as follows:

$$\sigma^2 = \frac{1}{N}\sum_{i,j}(h(i,j)-\bar{h})^2, \qquad (7)$$

where $N$ is the number of sites on the substrate ; $h(i,j)$ is the height of the film above the (001) substrate lattice site $(i,j)$, which is defined as the height of the highest occupied lattice site, and $\bar{h}$ is the mean height of the thin film. The relative density of the film is calculated by averaging the ratio of the number of occupied sites to the total number of sites in the middle ten layers. The variations of roughness and density with incidence angle at different deposition rates are plotted in Figs.6 (a) and (b). For $\theta = 0°$, the density is close to 1.0, indicating that very few voids exist in the film in this situation. The roughness increases when the incidence angle becomes larger; meanwhile the density decreases. The reason is that some high columns and highly voided region are formed when the incidence angle gets larger. This is in agreement with the previous discussion. However, in the case of larger $\theta$ (60° and 75°), the roughness decreases slightly. The reason is that when $\theta$ is larger, the upper columns overlap the layers below. In this case, the roughness $\sigma$ cannot really describe the surface roughness. This can be seen from Fig.4 (b), where the columns stretch out above and overlap the film.

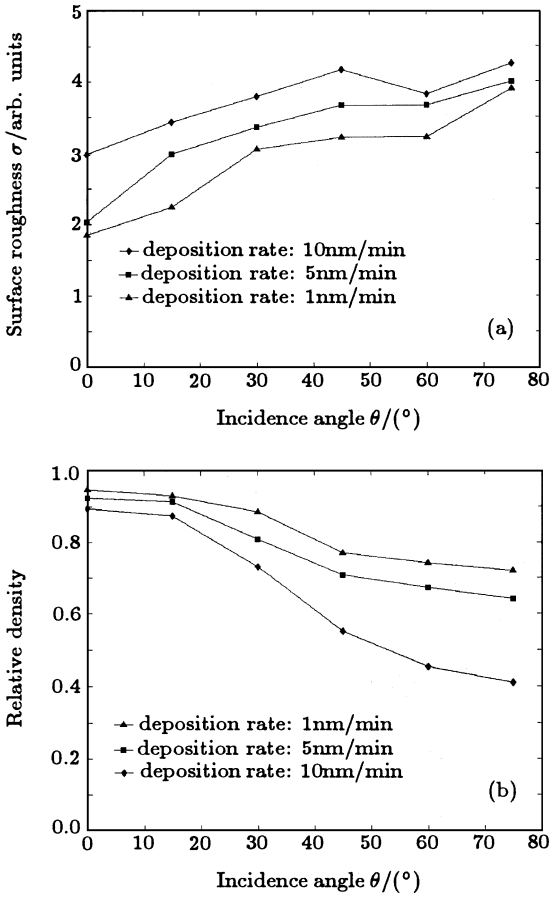



**Fig.6.** The plots of (a) surface roughness and (b) density of the film variations with incidence angle; $\theta = 0°, 15°, 30°, 60°$ and 75° at different deposition rates.

# 4. Conclusion

We have developed a 3D model to simulate Cu film growth based on the KMC method. The 3D morphology and microstructures of Cu films have been investigated in our model, in which the existence of the over-hangs is considered but not allowed in the earlier model. The main goal of the simulation is to investigate the effect of incidence angle on the morphology of the films. The results show that the columnar structure is affected by the incidence angle of the atoms. The columns are connected to each other at a small incidence angle. When the incidence angle is large enough, the columns are completely separated by a few large void regions. The columns are inclined toward the direction of the incidence angle and the inclined angles become larger when the incidence angles are larger. The simulation results are in good agreement with experimental results.[22,23] However, in our

simulations, the relation of the inclined angles and the incidence angle is not completely consistent with the tangent rule. The reason is that the over-hangs at the step edge can result in small inclined angles.

## Acknowledgement

The authors thank Dr W. D. Zou for helpful discussions

## References

[1] Scorzoni A *et al* 1991 *Mater. Sci. Rep.* **7** 143
[2] Macleod H A 1986 *J. Vac. Sci. Technol.* A **4** 418
[3] Motohiro T and Taga Y 1989 *Appl. Opt.* **28** 2466
[4] Witten T A and Sender M 1981 *Phys. Rev. Lett.* **47** 400
[5] Bruschi P *et al* 1997 *Phys. Rev.* B **55** 7955
[6] Wei H L, Liu Z L and Yao K L 1999 *Acta Phys. Sin.* **48** 1302 (in Chinese)
[7] Wei H L, Liu Z L and Yao K L 2000 *Acta Phys. Sin.* **49** 791 (in Chinese)
[8] Chen M, Wei H L and Liu Z L 2001 *Acta Phys. Sin.* **50** 2446 (in Chinese)
[9] Kotrla M 1996 *Comput. Phys. Comm.* **97** 82
[10] Smy T *et al* 1998 *IEEE Trans. Comput. Aided Des.* **10** 130
[11] Meakin P *et al* 1986 *Phys. Rev.* A **34** 5091
[12] Huang H C, Gilmer G H and Rubia T D de La 1998 *J. Appl. Phys.* **84** 3636
[13] Gilmer G H, Huang H C and Rubia T D de La 2000 *Thin Solid Films* **365** 189
[14] Abelman L and Lodder C 1997 *Thin Solid Films* **305** 1
[15] Levine S W *et al* 1998 *Surf. Sci.* **401** 112
[16] Breeman M *et al* 1996 *Thin Solid Films* **272** 195
[17] Rosato V *et al* 1989 *Philos. Mag.* A **59** 321
[18] Ju S P *et al* 2002 *J. Appl. Phys.* **92** 7062
[19] Dirks A G *et al* 1977 *Thin Solid Films* **47** 219
[20] Torre J D *et al* 2003 *J. Appl. Phys.* **94** 263
[21] Nieuwenhuizen J M *et al* 1966 *Philips Tech. Rev.* **27** 87
[22] Wei H L, Huang H C and Woo C H 2002 *Appl. Phys. Lett.* **80** 2290
[23] Huang H C, Wei H L and Woo C H 2002 *Appl. Phys. Lett.* **81** 4359